Supporting Information

From Crystalline to Amorphous: Heterostructure Design of MoO_2/MoS_2 In-situ Supported by Nitrogen-doped Carbon with Robust Sodium Storage at -40 °C

Shaocong Tang[a], Jiabao Li[a]*, Ziqian Li[a], Jingjing Hao[a], Tianyi Wang[a], Likun Pan[b]*, Chengyin Wang[a]*

[a]School of Chemistry and Chemical Engineering, Yangzhou University, 180 Si-Wang-Ting Road, Yangzhou, Jiangsu 225002, China

[b]Shanghai key laboratory of Magnetic Resonance, School of Physics and Electronic Science, East China Normal University, Shanghai 200241, China

Corresponding Authors: jiabaoli@yzu.edu.cn (Jiabao Li); lkpan@phy.ecnu.edu.cn (Likun Pan); wangcy@yzu.edu.cn (Chengyin Wang)

Material Characterizations

The structure and morphology of as-fabricated samples were investigated through the field-emission scanning electron microscope (FESEM, Hitachi-4800) and transmission electron microscopy (TEM, Tecnai G2 F30). The amorphous structure was confirmed by the X-ray powder diffraction (XRD, Bruker-D8 ADVANCE). Raman spectra were collected on RM-1000 (Renishaw In Via), and the surface chemical component was characterized through the X-ray photoelectron spectrometry (XPS, Thermo ESCALAB 250 XI). The amounts of carbon and nitrogen in the final products were evaluated by using elementary CHN combustion analysis. The content of sulfur in the materials was measured through ICP–OES (Spectro Arcos).

Electrochemical Measurements

The working electrode containing as-fabricated active materials (a-MoO_2/MoS_2@NC or c-MoO_2/MoS_2@NC), conductive agent (acetylene black), as well as the binder (carboxymethyl cellulose) was added to the deionized water with a mass ratio of 8:1:1, and then grounded to form a uniform slurry, which was further coated on a copper foil and dried at 100 °C for 24 h. For the cells assembled in an argon-filled glovebox (oxygen and water contents less than 0.1 ppm), sodium foil was used as the counter and reference electrode, and Whatman glass fiber was employed as the separator, and the electrolyte is 1.0 M NaClO4 dissolved in ethylene carbonate and propylene carbonate (weight ratio 1:1) add with 5.0 wt.% fluoroethylene carbonate. The galvanostatic discharging/discharging tests were conducted on a Neware BTS-4000 battery test system in a voltage range of 0.05-3.0 V at various current densities.

Galvanostatic intermittent titration technique (GITT) measurements were carried out at a current density of 50 mA g^{-1} in the intermittent charge mode with a rest period of 2 h. Cyclic voltammetry (CV) and electrochemical impedance spectroscopy (EIS) of the electrodes were implemented on a CHI660E (Chenhua, China) electrochemical workstation.

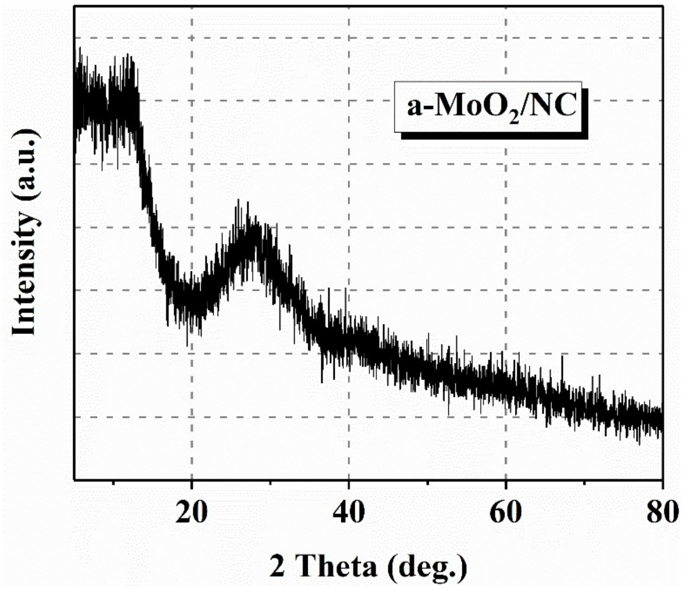

Fig. S1 XRD pattern of the a-MoO_2/NC.

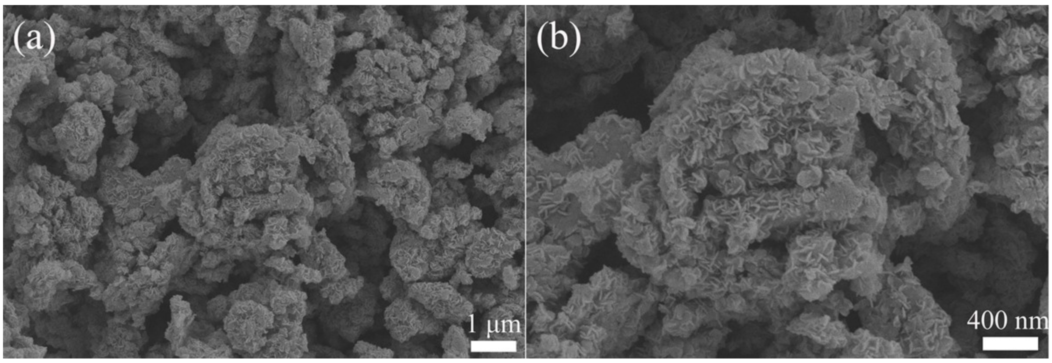

Fig. S2 FESEM images of the c-MoO_2/MoS_2@NC (a and b) with different magnifications.

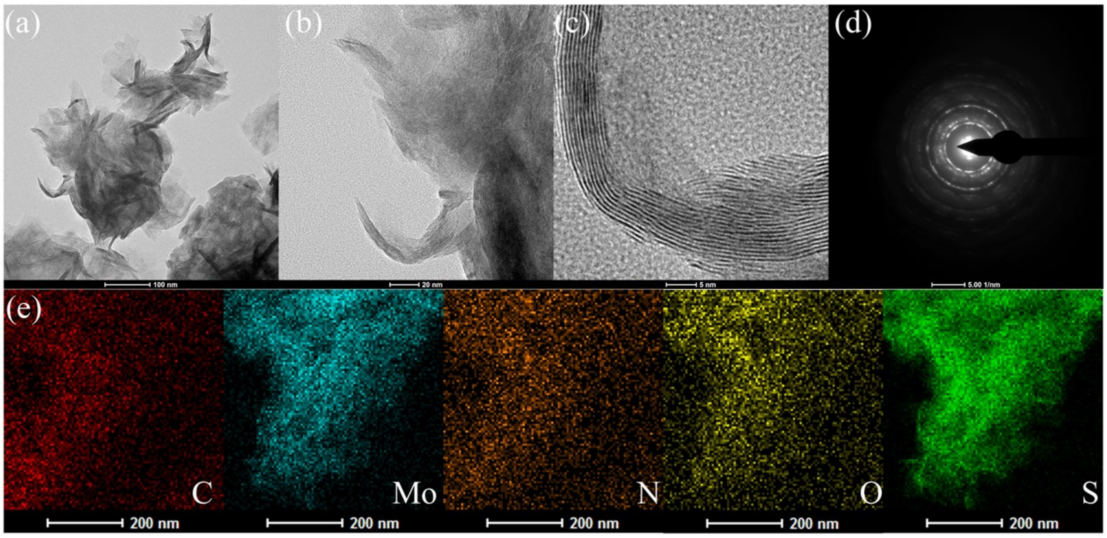

Fig. S3 TEM (a and b), HRTEM (c) images, SAED pattern (d), and elemental mapping (e) of c-MoO_2/MoS_2@NC.

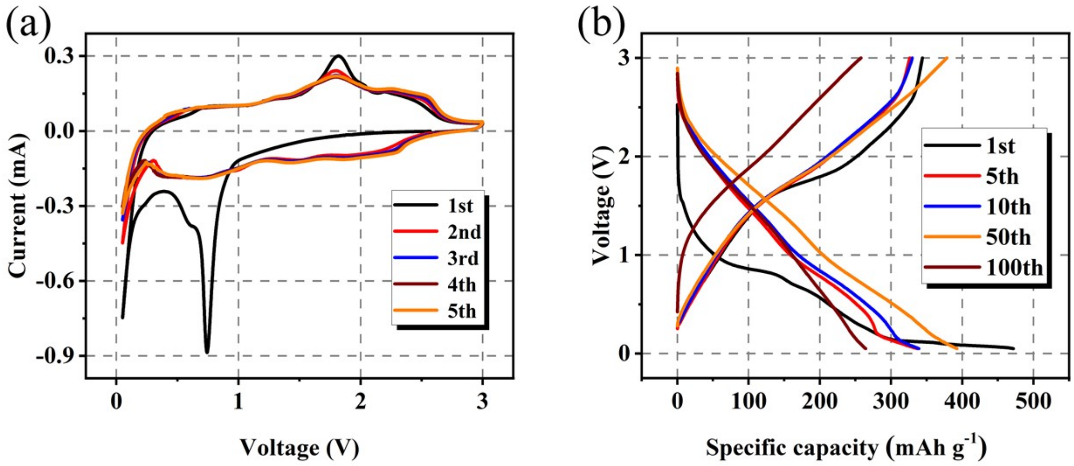

Fig. S4 CV curves (a) at 0.2 mV s^{-1} ranging from 0.05 to 3.0 V and discharging/charging profiles (b) of c-MoO_2/MoS_2@NC.

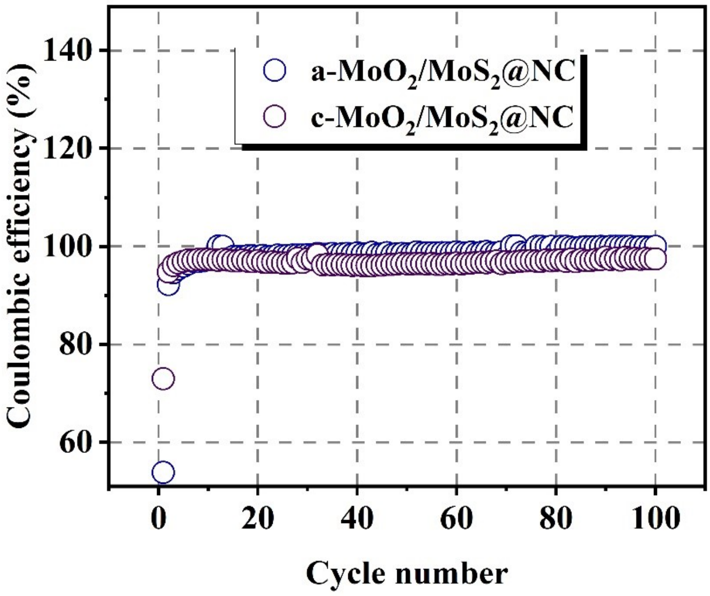

Fig. S5 Comparison of the Coulombic efficiencies of cycling at 0.1 A g^{-1} between a-MoO$_2$/MoS$_2$@NC and c-MoO$_2$/MoS$_2$@NC.

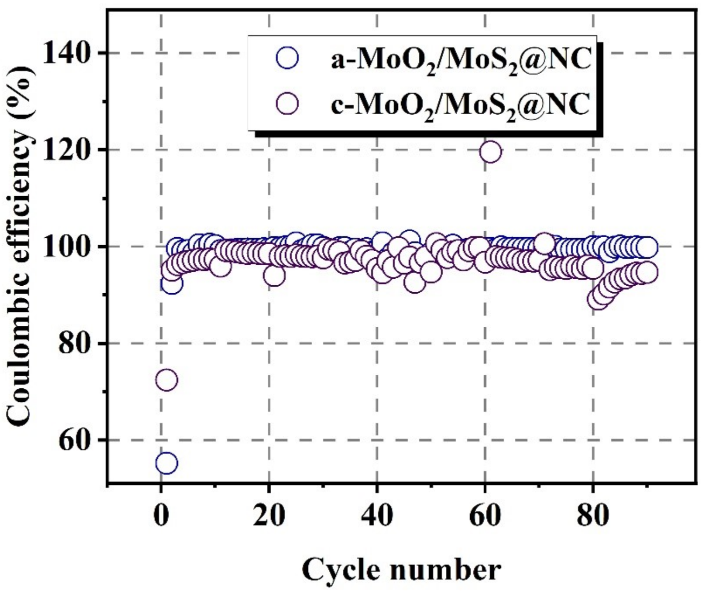

Fig. S6 Comparison of the Coulombic efficiencies of rate capabilities between a-MoO$_2$/MoS$_2$@NC and c-MoO$_2$/MoS$_2$@NC.

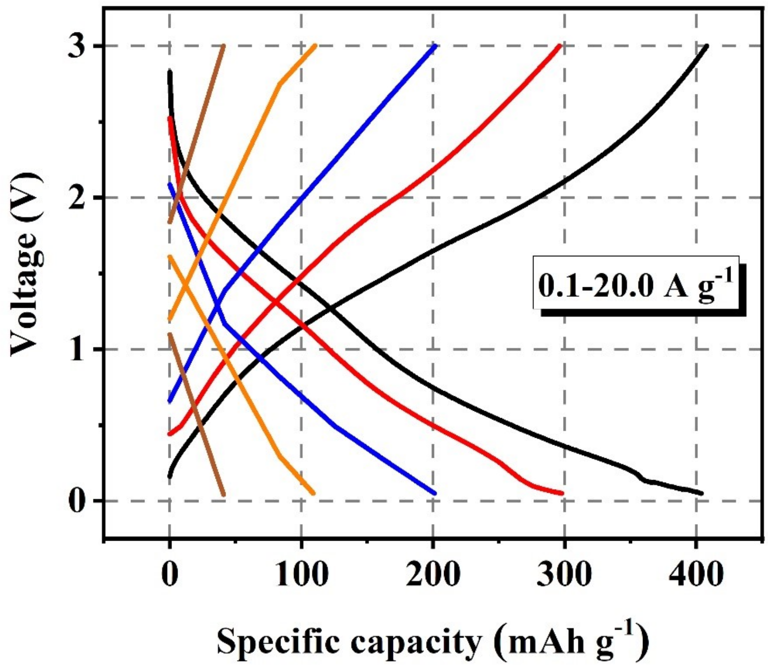

Fig. S7 Rate profiles of a-MoO_2/MoS_2@NC.

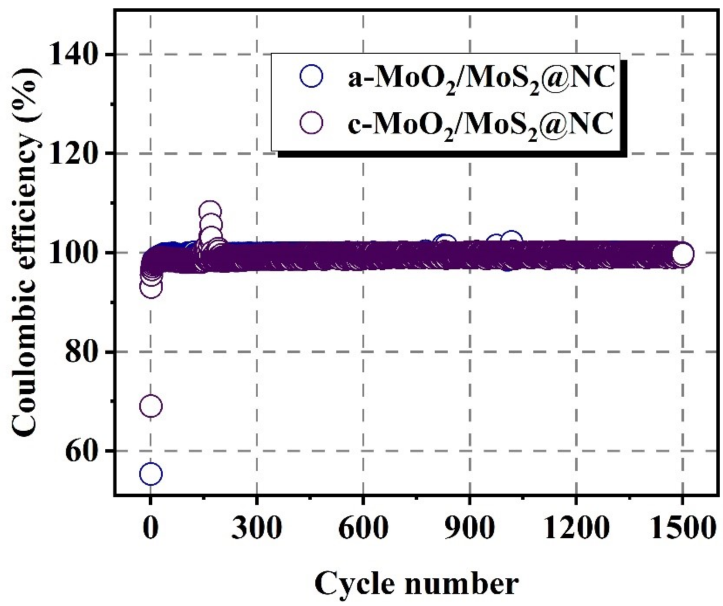

Fig. S8 Coulombic efficiencies of a-MoO_2/MoS_2@NC and c-MoO_2/MoS_2@NC at 1.0 A g^{-1}.

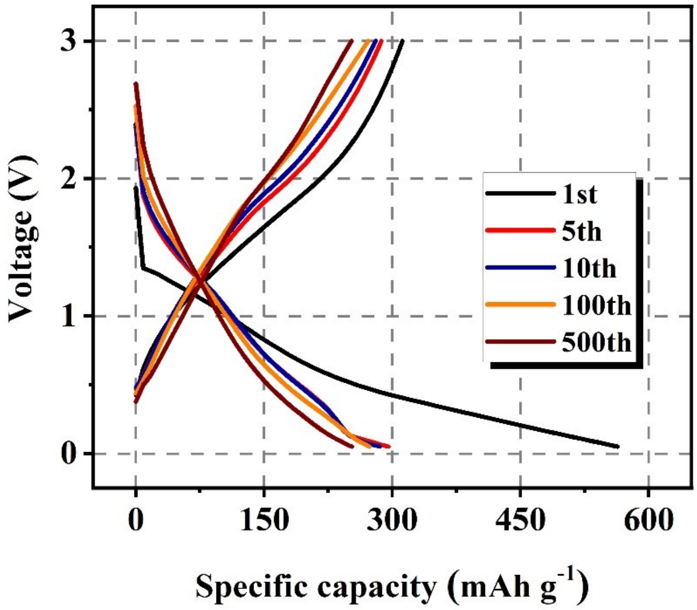

Fig. S9 Coulombic efficiencies of a-MoO_2/MoS_2@NC and c-MoO_2/MoS_2@NC at 1.0 A g^{-1}.

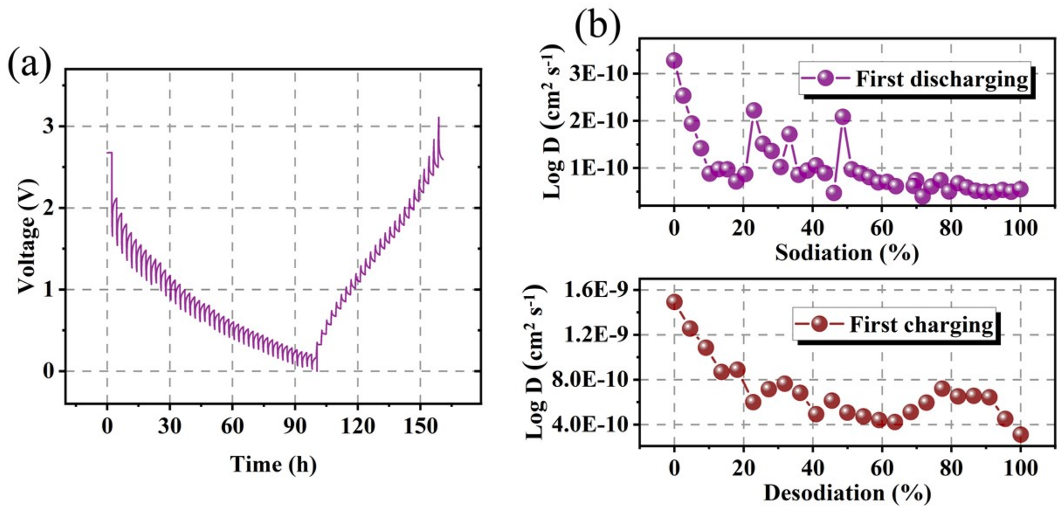

Fig. S10 Galvanostatic intermittent titration versus time curve (a), and ionic diffusion coefficients upon discharging and charging (b) for the c-MoO_2/MoS_2@NC electrode.

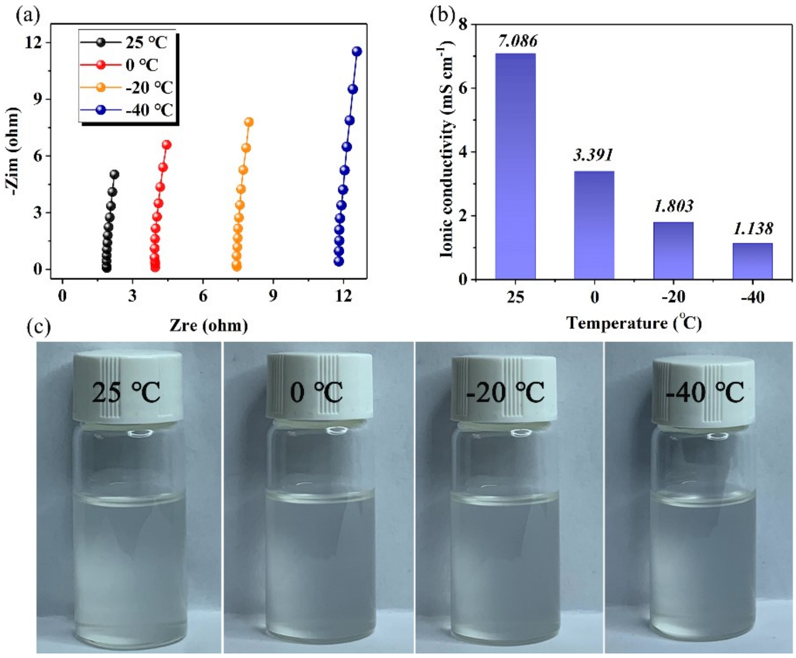

Fig. S11 Nyquist plots for the electrolyte employed at different temperatures (a). The ionic conductivities of electrolyte at various temperatures (b). The digital photos of the electrolyte at various temperatures (c).

Generally, the ionic conductivity of electrolyte can be estimated using a bipolar plate device, which contains two stainless steel plates and a separator soaked with electrolyte. Through the EIS measurements at various temperatures, the ionic conductivity at different temperatures can be determined based on the following formula:

$$\sigma = \frac{h}{R \times S}$$

where σ is the ionic conductivity, h is the distance between tow plates, R is the resistance of electrolyte, and S is the surface area of the plate.

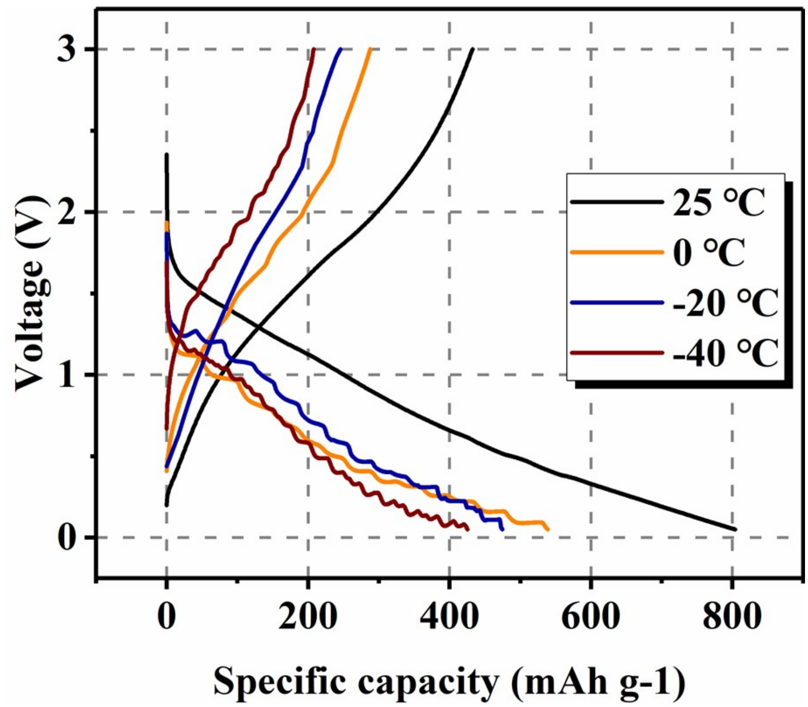

Fig. S12 The comparison of initial discharge/charge profiles of target a-MoO2/MoS2@NC at 25, 0, -20 and -40 °C.

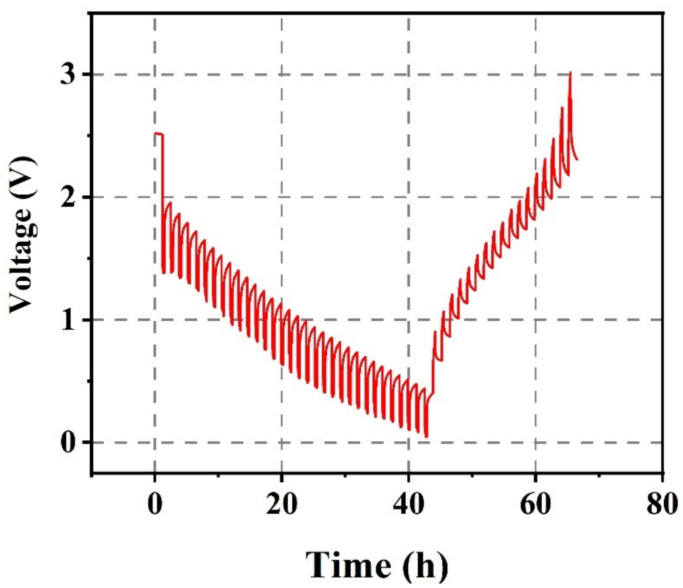

Fig. S13 Galvanostatic intermittent titration versus time curve of the a-MoO_2/MoS_2@NC electrode at 0 °C.

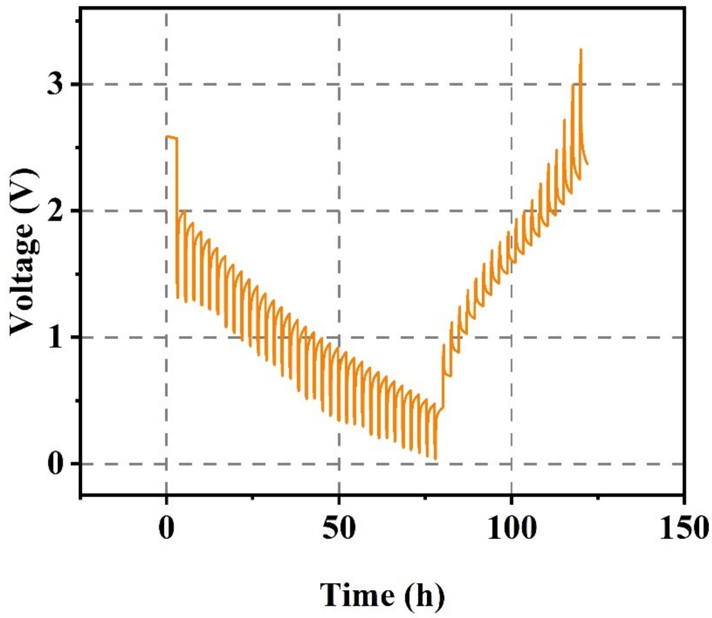

Fig. S14 Galvanostatic intermittent titration versus time curve of the a-MoO_2/MoS_2@NC electrode at -20 °C.

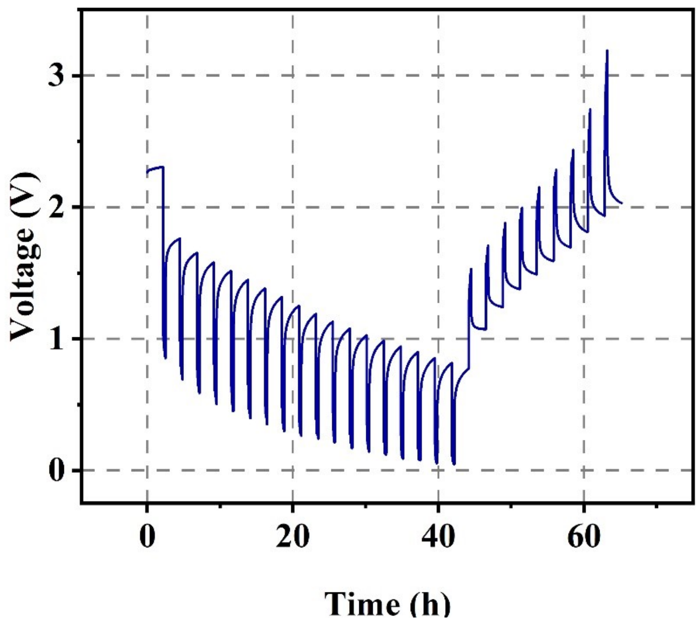

Fig. S15 Galvanostatic intermittent titration versus time curve of the a-MoO_2/MoS_2@NC electrode at -40 °C.

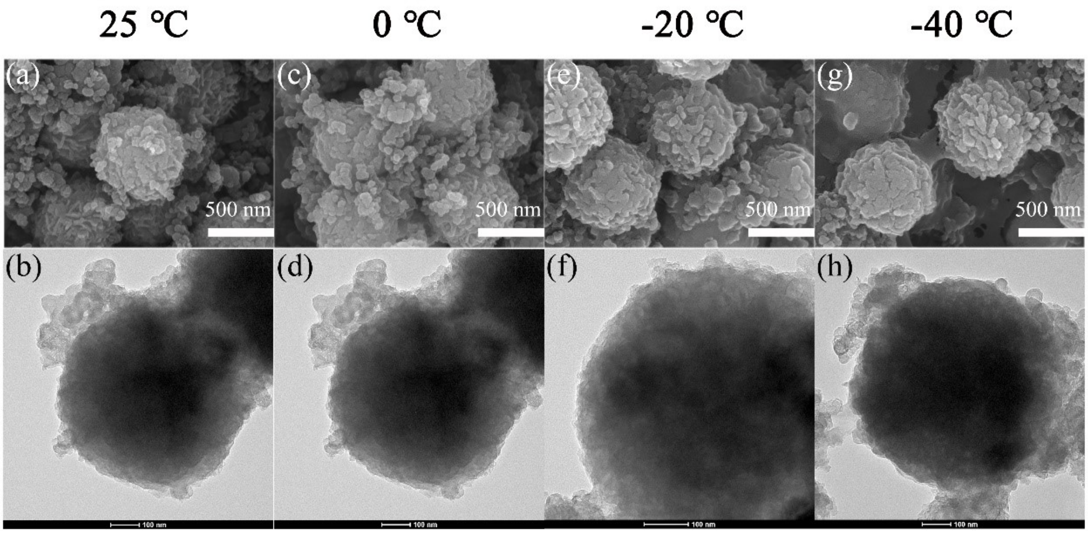

Fig. S16 The SEM and TEM characterizations of a-MoO_2/MoS_2/NC after 100 cycles at 0.1 A g^{-1} at 25 (a and b), 0 (c and d), -20 (e and f) and -40 (g and h) °C.

Table S1 Element analysis report of a-MoO_2@MoS_2@NC and the calculation equations for the mass fractions of MoS_2 and MoO_2 components, respectively.

a-MoO_2/MoS_2@NC	N[a]	C[a]	H[a]	S[b]
Content (wt.%)	3.46	15.36	0.48	16.32

[a] Estimated by CHN analysis. [b] Obtained from ICP-OES measurement.

$$W\ wt.\%(MoS_2) = (W\ wt.\%(S)*M(MoS2))/2M(S)=45.82\ wt.\%$$

$$W\ wt.\%(MoO_2) =1-W\ wt.\%(N) - W\ wt.\%(C) - W\ wt.\%(H) - W\ wt.\%(MoS_2) = 34.88\ wt.\%$$

Table S2 The comparison of sodium storage performance of as-prepared a-MoO_2/MoS_2@NC with other related materials at room temperature.

Samples	Voltage range (V)	Cycling performance	Rate capability	Ref.
MoO_2 nanosheets@carbon fiber	0.01-3.0	223.6 mAh g^{-1} after 100 cycles at 0.1 A g^{-1}	284.8 mAh g^{-1} at 0.05 A g^{-1} 256.7 mAh g^{-1} at 0.1 A g^{-1} 226.2 mAh g^{-1} at 0.2 A g^{-1} 197.2 mAh g^{-1} at 0.5 A g^{-1} 169.6 mAh g^{-1} at 1.0 A g^{-1} 137.5 mAh g^{-1} at 2.0 A g^{-1}	1
TiO_2@MoO_2-Carbon matrix	0.01-3.0	210 mAh g^{-1} after 500 cycles at 1.0 A g^{-1}	About 287.0 mAh g^{-1} at 0.05 A g^{-1} ～276.2 mAh g^{-1} at 0.1 A g^{-1} About 262.5 mAh g^{-1} at 0.2 A g^{-1} About 237.6 mAh g^{-1} at 0.5 A g^{-1} About 225.5 mAh g^{-1} at 1.0 A g^{-1} About 201.2 mAh g^{-1} at 2.0 A g^{-1} About 175.3 mAh g^{-1} at 3.0 A g^{-1} About 158.9 mAh g^{-1} at 5.0 A g^{-1} About 125.2 mAh g^{-1} at 8.0 A g^{-1} About 110.0 mAh g^{-1} at 10.0 A g^{-1} About 95.2 mAh g^{-1} at 15.0 A g^{-1} About 76.0 mAh g^{-1} at 20.0 A g^{-1}	2

MoO_2/C nanosheets	0.01-3	306.0 mAh g^{-1} after 50cycles at 0.1 A g^{-1}	331.0 mAh g^{-1} at 0.2 A g^{-1} 224.0 mAh g^{-1} at 0.5 A g^{-1} 164.1 mAh g^{-1} at 1.0 A g^{-1} 105.0 mAh g^{-1} at 2.0 A g^{-1} 52.5 mAh g^{-1} at 5.0 A g^{-1}	3
MoO_2/3D porous carbon	0.01-3	About 367.0 mAh g^{-1} after 200 cycles at 0.1 A g^{-1}	About 380.2 mAh g^{-1} at 0.1 A g^{-1} About 356.3 mAh g^{-1} at 0.2 A g^{-1} About 289.3 mAh g^{-1} at 0.5 A g^{-1} About 238.6 mAh g^{-1}at 1.0 A g^{-1} About 211.1 mAh g^{-1} at 2.0 A g^{-1}	4
MoS_2/graphite composite	0.01-3	About 254.0 mAh g^{-1} after 800 cycles at 0.1 A g^{-1}	267.8 mAh g^{-1} at 0.05 A g^{-1} 250.9 mAh g^{-1} at 0.1 A g^{-1} 264.4 mAh g^{-1} at 0.2 A g^{-1} 231.9 mAh g^{-1} at 0.5 A g^{-1} 225.4 mAh g^{-1} at 1.0 A g^{-1}	5
Mo-defect-rich ultrathin MoS_2	0.01-3	384.3 mAh g^{-1} after 100 cycles at 0.1 A g^{-1}	412.0 mAh g^{-1} at 0.1 A g^{-1} 381.0 mAh g^{-1} at 0.2 A g^{-1} 317.0 mAh g^{-1} at 0.5 A g^{-1} 291.0 mAh g^{-1} at 1.0 A g^{-1} 266.0 mAh g^{-1} at 2.0 A g^{-1} 226.0 mAh g^{-1}at 5.0 A g^{-1}	6

Cu_2S@carbon@MoS_2	0.01-3	297.0 mAh g^{-1} after 200 cycles at 3.0 A g^{-1}	430.0 mAh g^{-1} at 0.05 A g^{-1} 410.0 mAh g^{-1} at 0.1 A g^{-1} 386.0 mAh g^{-1} at 0.2 A g^{-1} 368.0 mAh g^{-1} at 0.3 A g^{-1} 359.0 mAh g^{-1} at 0.5 A g^{-1} 337.0 mAh g^{-1} at 1.0 A g^{-1} 316.0 mAh g^{-1} at 2.0 A g^{-1}	[7]
1T MoS_2-graphene-MoS_2	0.01-3	313.0 mAh g^{-1} after 200 cycles at 0.05 A g^{-1}	241.0 mAh g^{-1} at 0.5A g^{-1} 222.0 mAh g^{-1} at 0.8 A g^{-1} 208.0 mAh g^{-1} at 1.0 A g^{-1} 190.0 mAh g^{-1} at 1.5 A g^{-1} 175.0 mAh g^{-1} at 2.0 A g^{-1}	[8]
$MoS_2/Ti_3C_2T_x$ composite	0.01-3	250.9 mAh g^{-1} after 100 cycles at 0.1 A g^{-1}	392.6 mAh g^{-1} at 0.05 A g^{-1} 285.4 mAh g^{-1} at 0.1 A g^{-1} 245.6 mAh g^{-1} at 0.2 A g^{-1} 207.2 mAh g^{-1} at 0.5 A g^{-1} 162.7 mAh g^{-1} at 1.0 A g^{-1}	9[9]
oxygen-incorporated MoS_2/carbon fiber	0.01-3	330.0 mAh g^{-1} after 100 cycles at 0.1 A g^{-1}	288.0 mAh g^{-1} at 0.2 A g^{-1} 268.0 mAh g^{-1} at 0.3 A g^{-1} 241.0 mAh g^{-1} at 0.5 A g^{-1} 225.0 mAh g^{-1} at 1.0 A g^{-1}	[10]

MoO_2@MoS_2/reduced graphene oxide	0.01-3	362.5 mAh g^{-1} after 300 cycles at 1.0 A g^{-1}	496.8 mAh g^{-1} at 0.1 A g^{-1} 463.5 mAh g^{-1} at 0.2 A g^{-1} 425.2 mAh g^{-1} at 0.5 A g^{-1} 408.6 mAh g^{-1} at 1.0 A g^{-1} 390.6 mAh g^{-1} at 2.0 A g^{-1} 361.2 mAh g^{-1} at 5.0 A g^{-1} 334.7 mAh g^{-1} at 10.0 A g^{-1}	11
MoO_2@MoS_2/nitrogen -doped carbon nanorods	0.01-3	435.2 mAh g^{-1} after 100 cycles at 0.2 A g^{-1}	About 422.2 mAh g^{-1} at 0.2 A g^{-1} About 401.3 mAh g^{-1} at 0.5 A g^{-1} About 395.3 mAh g^{-1} at 1.0 A g^{-1} About 358.6 mAh g^{-1}at 3.0 A g^{-1} About 330.1 mAh g^{-1} at 5.0 A g^{-1}	12
a-MoO_2/MoS_2@nitrogen -doped carbon	0.05-3	406.8 mAh g^{-1} after 100 cycles at 0.1 A g^{-1}	410.1 mAh g^{-1} at 0.1 A g^{-1} 345.2 mAh g^{-1} at 1.0 A g^{-1} 201.6 mAh g^{-1} at 5.0 A g^{-1} 114.7 mAh g^{-1} at 10.0 A g^{-1} 41.5 mAh g^{-1} at 20.0 A g^{-1}	This work

Table S3 The comparison of initial discharge/charge capacities and initial Coulombic efficiency of a-MoO_2@MoS_2@NC at various temperatures.

Operating temperature (°C)	Initial discharge capacity (mAh g^{-1})	Initial charge capacity (mAh g^{-1})	Initial Coulombic efficiency (%)
25	803.8	432.5	53.8
0	538.8	287.8	53.4
-20	474.7	245.9	51.8
-40	425.2	207.7	48.8

Table S4 The comparison of sodium storage performance between the as-prepared a-MoO_2/MoS_2@NC and the other reported materials at low temperatures.

Samples	Voltage range (V)	Cycling performance at low temperature	Rate capability at low temperature
$NaTi_2(PO_4)_3$/Carbon [13]	1.5-3.0	98.5 mAh g^{-1} after 200 cycles at 0.5 A g^{-1} at 0℃ 94.3 mAh g^{-1} after 200 cycles at 0.5 A g^{-1} at -25℃	101.7 mAh g^{-1} at 0.5 A g^{-1} 97.5 mAh g^{-1} at 2.0 A g^{-1} 95.0 mAh g^{-1} at 4.0A g^{-1} 88.2 mAh g^{-1} at 6.0 A g^{-1} 81.3 mAh g^{-1} at 8.0 A g^{-1} at 0 °C
a-$KTiO_x$/Ti_2CT_x [14]	0.005-3.0	144.2 mAh g^{-1} after 100 cycles at 0.1 A g^{-1} at 0℃ 112.6 mAh g^{-1} after 100 cycles at 0.1 A g^{-1} at -25℃	152.1 mAh g^{-1} at 0.1 A g^{-1} 110.8 mAh g^{-1} at 0.5 A g^{-1} 70.1 mAh g^{-1} at 2.0A g^{-1} 56.8 mAh g^{-1} at 4.0 A g^{-1} at 0 °C
Two-dimensional NbSSe nanoplates [15]	0.05-3.0	136.0 mAh g^{-1} after 50 cycles at 0.3 A g^{-1} at 0℃ About 72.6 mAh g^{-1} after 50 cycles at 0.3 A g^{-1} at -25℃	145.0 mAh g^{-1} at 0.1 A g^{-1} 133.3 mAh g^{-1} at 0.2 A g^{-1} 122.5 mAh g^{-1} at 0.5 A g^{-1} 112.4 mAh g^{-1} at 1.0 A g^{-1} 103.8 mAh g^{-1} at 2.0A g^{-1} 85 mAh g^{-1} at 3.0A g^{-1} at 0 °C

NiO nanosheet@nitrogen-doped carbon [16]	0.005-3.0	/	About 58.1 mAh g^{-1} at 0.05 A g^{-1} About 42.2 mAh g^{-1} at 0.1 A g^{-1} About 37.1 mAh g^{-1} at 0.2 A g^{-1} About 34.1 mAh g^{-1} at 0.4 A g^{-1} About 33.2 mAh g^{-1} at 0.8 A g^{-1} About 313 mAh g^{-1} at 1.0 A g^{-1} About 30.1 mAh g^{-1} at 2.0 A g^{-1} About 30.0 mAh g^{-1} at 4.0 A g^{-1} at -25℃
$NaTi_2(PO_4)_3$/carbon-carbon nanotubes [17]	1.5-3.0	117.9 mAh g^{-1} at 0.5 A g^{-1} at 0℃ 17.1 mAh g^{-1} at 0.5 A g^{-1} at -10℃	/
TiO_2-B/anatase dual-phase nanowire [18]	0.01-3.0	About 10 mAh g^{-1} after 100 cycles at 1.0 A g^{-1} at 0℃	About 161.1 mAh g^{-1} at 0.25 A g^{-1} About 152.2 mAh g^{-1} at 0.5 A g^{-1} About 147.1 mAh g^{-1} at 1.0 A g^{-1} About 138.1 mAh g^{-1} at 2.0 A g^{-1} About 131.2 mAh g^{-1} at 5.0 A g^{-1} About 127.3 mAh g^{-1} at 10.0 A g^{-1} About 127.1 mAh g^{-1} at 20.0 A g^{-1} at 0℃
$Fe_{1-x}S$ nanosheet@nitrogen-doped carbon [19]	0.01-3.0	/	467.1 mAh g^{-1} at 0.1 A g^{-1} 369.3 mAh g^{-1} at 0.5 A g^{-1} 300.5 mAh g^{-1} at 1.0 A g^{-1} 223.4 mAh g^{-1} at 2.0 A g^{-1} 193.8 mAh g^{-1} at 2.5A g^{-1} 159.9 mAh g^{-1} at 3.0A g^{-1} at -20 °C

Nano $NaTi_2(PO_4)_3$@ Carbon [20]	1.5-3.0	100.05 mAh g^{-1} after 200 cycles at 0.2 A g^{-1} at -20 °C	109.0 mAh g^{-1} at 1.0 A g^{-1} 99.0 mAh g^{-1} at 2.0 A g^{-1} 92.0 mAh g^{-1} at 5.0 A g^{-1} 72.0 mAh g^{-1} at 10.0 A g^{-1} at -20 °C
a-MoO2/MoS2 @NC This work	0.005-3.0	302.5 mAh g^{-1} after 100 cycles at 0.1 A g^{-1} at -0 °C 151.7 mAh g^{-1} after 100 cycles at 0.1 A g^{-1} at -40 °C	298.3 mAh g^{-1} at 0.1 A g^{-1} 216.5 mAh g^{-1} at 0.5 A g^{-1} 145.7 mAh g^{-1} at 1.0 A g^{-1} 82.6 mAh g^{-1} at 2.0 A g^{-1} 43.5 mAh g^{-1} at 4.0 A g^{-1} at 0 °C

Reference

1. H. Zhang, Z. Han, X. Li, F. Kong, S. Tao and B. Qian, MoO_2 nanosheets embedded into carbon nanofibers with a self-standing structure for lithium ion and sodium ion batteries, *Ceram. Int.*, 2021, **47**, 26839-26846.
2. C. Zhao, C. Yu, M. Zhang, H. Huang, S. Li, X. Han, Z. Liu, J. Yang, W. Xiao, J. Liang, X. Sun and J. Qiu, Ultrafine MoO_2-Carbon Microstructures Enable Ultralong-Life Power-Type Sodium Ion Storage by Enhanced Pseudocapacitance, *Adv. Energy Mater.*, 2017, **7**, 1602880.
3. J. Jiang, W. Yang, H. Wang, Y. Zhao, J. Guo, J. Zhao, M. Beidaghi and L. Gao, Electrochemical Performances of MoO_2/C Nanocomposite for Sodium Ion Storage: An Insight into Rate Dependent Charge/Discharge Mechanism, *Electrochim. Acta*, 2017, **240**, 379-387.
4. S. Bao, S.-h. Luo, S.-x. Yan, Z.-y. Wang, Q. Wang, J. Feng, Y.-l. Wang and T.-f. Yi, Nano-sized MoO_2 spheres interspersed three-dimensional porous carbon composite as advanced anode for reversible sodium/potassium ion storage, *Electrochim. Acta*, 2019, **307**, 293-301.
5. Q. Yang, M. Liu, Y. Hu, Y. Xu, L. Kong and L. Kang, Facile synthesis of MoS_2/graphite intercalated composite with enhanced electrochemical performance for sodium ion battery, *J. Energy Chem.*, 2018, **27**, 1208-1213.
6. Y. Li, R. Zhang, W. Zhou, X. Wu, H. Zhang and J. Zhang, Hierarchical MoS_2 Hollow Architectures with Abundant Mo Vacancies for Efficient Sodium Storage, *ACS Nano*, 2019, **13**, 5533-5540.

7. Y. Fang, D. Luan, Y. Chen, S. Gao, and X. W. Lou, Rationally Designed Three-Layered Cu_2S@Carbon@MoS_2 Hierarchical Nanoboxes for Efficient Sodium Storage, *Angew. Chem. Int. Ed*., 2020, **59**, 7178-7183.

8. X. Geng, Y. Jiao, Y. Han, A. Mukhopadhyay, L. Yang and H. Zhu, Freestanding Metallic 1T MoS_2 with Dual Ion Diffusion Paths as High Rate Anode for Sodium-Ion Batteries, *Adv. Funct. Mater.*, 2017, **27**, 1702998.

9. Y. Wu, P. Nie, J. Jiang, B. Ding, H. Dou and X. Zhang, MoS_2-Nanosheet-Decorated 2D Titanium Carbide (MXene) as High-Performance Anodes for Sodium-Ion Batteries, *ChemElectroChem*, 2017, **4**, 1560-1565.

10. Y. Zhang, H. Tao, T. Li, S. Du, J. Li, Y. Zhang and X. Yang, Vertically Oxygen-Incorporated MoS_2 Nanosheets Coated on Carbon Fibers for Sodium-Ion Batteries, *ACS Appl. Mater. Interface*, 2018, **10**, 35206-35215.

11. Y. Luo, X. Ding, X. Ma, D. Liu, H. Fu and X. Xiong, Constructing MoO_2@MoS_2 Heterostructures anchored on graphene nanosheets as a high-performance anode for sodium ion batteries, *Electrochim. Acta*, 2021, **388**, 138612.

12. W. Yang, L. Han, X. Liu, L. Hong and M. Wei, Template-free fabrication of 1D core-shell MoO_2@MoS_2/nitrogen-doped carbon nanorods for enhanced lithium/sodium-ion storage, *J. Colloid Interface Sci.*, 2021, **588**, 804-812.

13. J. Li, Z. Li, S. Tang, T. Wang, K. Wang, L. Pan and C. Wang, Sodium titanium phosphate nanocube decorated on tablet-like carbon for robust sodium storage performance at low temperature, *J. Colloid Interface Sci.*, 2023, **629**, 121-132.

14. J. Li, S. Tang, Z. Li, Z. Ding, T. Wang and C. Wang, Cross-linked amorphous potassium titanate Nanobelts/Titanium carbide MXene nanoarchitectonics for efficient sodium storage at low temperature, *J. Colloid Interface Sci.*, 2023, **629**, 461-472.

15. L.-F. Zhou, X.-W. Gao, T. Du, H. Gong, L.-Y. Liu and W.-B. Luo, Two-Dimensional NbSSe as anode material for low-temperature sodium-ion batteries, *Chem. Eng. J.*, 2022, **435**, 134838.

16. Z. Bai, X. Lv, D. H. Liu, D. Dai, J. Gu, L. Yang and Z. Chen, Two-Dimensional NiO@C-N Nanosheets Composite as a Superior Low-Temperature Anode Material for Advanced

Lithium-/Sodium-Ion Batteries, *ChemElectroChem*, 2020, **7**, 3616-3622.

17. L. Wang, B. Wang, G. Liu, T. Liu, T. Gao and D. Wang, Carbon nanotube decorated $NaTi_2(PO_4)_3$/C nanocomposite for a high-rate and low-temperature sodium-ion battery ande, *RSC Adv*., 2016, **6**, 70277-70283.

18. D. Lin, K. Li, Q. Wang, L. Lyu, B. Li and L. Zhou, Rate-independent and ultra-stable low-temperature sodium storage in pseudocapacitive TiO_2 nanowires, *J. Mater. Chem. A*, 2019, **7**, 19297-19304.

19. H. Fan, B. Qin, Z. Wang, H. Li, J. Guo, X. Wu and J. Zhang, Pseudocapacitive sodium storage of $Fe_{1-x}S$@N-doped carbon for low-temperature operation, *Sci. China Mater.*, 2019, **63**, 505-515.

20. X. Zhang, M. Zeng, Y. She, X. Lin, D. Yang, Y. Qin and X. Rui, Enhanced low-temperature sodium storage kinetics in a $NaTi_2(PO_4)_3$@C nanocomposite, *J. Power Sources*, 2020, **477**, 228735.